

Cite this: *Chem. Sci.*, 2023, 14, 9154

All publication charges for this article have been paid for by the Royal Society of Chemistry

# A binuclear guanidinate yttrium carbyne complex: unique reactivity toward unsaturated C–N, C–O and C–S bonds†

Wen Jiang,<sup>‡a</sup> Feng Kong,<sup>‡a</sup> Iker del Rosal,<sup>‡a</sup> Meng Li,<sup>‡b</sup> Kai Wang,<sup>a</sup> Laurent Maron<sup>‡\*b</sup> and Lixin Zhang<sup>‡\*a</sup>

A guanidinato-stabilized binuclear yttrium carbyne complex [(PhCH<sub>2</sub>)<sub>2</sub>NC(NC<sub>6</sub>H<sub>3</sub><sup>i</sup>Pr<sub>2</sub>-2,6)<sub>2</sub>Y<sub>2</sub>(μ<sub>2</sub>-Me)(AlMe<sub>3</sub>)<sub>2</sub>(μ<sub>4</sub>-CH) (**1**) was synthesized via C–H bond activation and its versatile reactivities were investigated. Complex **1** underwent σ-bond metathesis with PhSSPh and nucleophilic addition with PhCN to form the corresponding yttrium thiolate complex **3** and aza-allyl complex **4** respectively. Additionally, the rare yttrium carbide complex **5** was also prepared by treatment of complex **1** with S<sub>8</sub>. Interestingly, in the reaction with PhNCS, the C=S double bond was cleaved, followed by C–H bond activation to give the yttrium sulfide complex **7** with a ketenimine dianion ligand. Unexpectedly, the reaction of complex **1** with CO (1 atm) resulted in deoxygenative coupling of CO, to afford mono- or dioxo-yttrium complexes at different temperatures. The mechanism of the possible formation processes of complexes **3** and **9** was elucidated by DFT calculations.

Received 7th July 2023  
Accepted 2nd August 2023

DOI: 10.1039/d3sc03483f

rsc.li/chemical-science

## Introduction

Since the first typical metal carbyne M≡CR (M = Cr, Mo, W) was reported,<sup>1</sup> transition-metal alkylidyne complexes have been extensively investigated because of their unique structural features and great potential in alkyne metathesis and stoichiometric reactions.<sup>2–4</sup> In stark contrast, the studies on the well-defined rare-earth-metal alkylidyne complexes are relatively limited.<sup>5–8</sup> This might be because the empty orbitals of rare-earth-metals are very high-energy d-orbitals and highly contracted f-orbitals, preventing the formation of strong covalent bonds with carbon atom orbitals. To date, four types of rare-earth-metal carbyne complexes have been successfully isolated and fully characterized. Firstly, Anwander *et al.* reported successfully a pentanuclear carbyne complex La<sub>5</sub>Al<sub>9</sub>(-CH)<sub>6</sub>(CH<sub>3</sub>)<sub>30</sub> (**A**) and tetranuclear carbyne complexes [(C<sub>5</sub>Me<sub>5</sub>)Y(μ<sub>2</sub>-Me)<sub>2</sub>AlMe]<sub>2</sub>(μ<sub>2</sub>-Me)(μ<sub>4</sub>-CH)<sub>2</sub> (**B**), La<sub>4</sub>Al<sub>8</sub>(CH)<sub>4</sub>(CH<sub>2</sub>)<sub>2</sub>(-CH<sub>3</sub>)<sub>20</sub>(PMe<sub>3</sub>) (**C**), and La<sub>4</sub>Al<sub>8</sub>(C)(CH)<sub>2</sub>(CH<sub>2</sub>)<sub>2</sub>(CH<sub>3</sub>)<sub>22</sub>(toluene) (**D**) via donor-induced alkylaluminates cleavage of hetero-

bimetallic Ln-(CH<sub>3</sub>)-Al linkages.<sup>6</sup> Subsequently, Mitzel and co-workers isolated the mononuclear Sm derivative [(TCyTAC)Sm<sup>III</sup>(μ<sub>4</sub>-CH)(AlMe<sub>3</sub>)<sub>3</sub>]<sup>7a,b</sup> (TCyTAC = 1,3,5-tricyclohexyl-1,3,5-triazacyclo-hexane) (**F**) and Pr derivative (η<sup>3</sup>-TMTAC)Pr(η<sup>4</sup>-{CH(AlMe<sub>3</sub>)<sub>3</sub>})<sup>7c</sup> (TMTAC = 1,3,5-trimethyl-1,3,5-triazacyclohexane) (**G**) through bulky base cyclic triamine initiated multiple C–H activation.

More recently, Cheng *et al.* discussed a rigid trinuclear scandium carbyne complex [(C<sub>5</sub>Me<sub>5</sub>)Sc(μ<sub>2</sub>-Br)]<sub>3</sub>(μ<sub>3</sub>-CH) (**E**) via methyl/halogenido exchange protocol of [(C<sub>5</sub>Me<sub>5</sub>)Sc(Me<sub>2</sub>)<sub>2</sub>]<sub>2</sub> with <sup>t</sup>BuBr.<sup>8</sup> However, a significant knowledge gap in the area involving binuclear rare-earth-metal alkylidyne complexes was incontrovertible. Additionally, compared to transition-metal alkylidyne complexes, the reactivity exploration of rare-earth-metal alkylidyne complexes remains scarce.<sup>8</sup>

In the last few decades, investigations on the synthesis and reactivity of rare-earth-metal alkylidyne complexes have been documented widely.<sup>9–15</sup> Our previous studies on amidinate rare-earth-metal carbene derivatives have also shown the unique reactivity of μ<sub>3</sub>-CH<sub>2</sub> dianions.<sup>16,17</sup> The results indicate that there are significant ligand effects on the structure and reactivity of these complexes. However, attempts to prepare guanidinate rare-earth-metal methylidyne complexes by a similar synthetic process for the synthesis of amidinate methylidyne complexes were unsuccessful, and an unexpected binuclear carbyne complex was isolated. Interestingly, this complex shows high and intriguing reactivity under mild conditions, which is distinct from those already reported for other transition-metal carbyne complexes.

<sup>a</sup>Department of Chemistry, Shanghai Key Laboratory of Molecular Catalysis and Innovative Materials, Fudan University, 2005 Songhu Road, Jiangwan Campus, Shanghai, 200438, P. R. China. E-mail: lixinzhang@fudan.edu.cn

<sup>b</sup>LPCNO, Université de Toulouse, 31077 Toulouse, France. E-mail: maron@irsamc.ups-tlse.fr

† Electronic supplementary information (ESI) available: Full experimental procedures, spectra, and analytical data. CCDC 2189939, 2189941–2189946 and 2262169. For ESI and crystallographic data in CIF or other electronic format see DOI: <https://doi.org/10.1039/d3sc03483f>

‡ These authors contributed equally to this work.



## Results and discussion

### Synthesis and structural characterization

The first binuclear yttrium carbyne complex  $[(\text{PhCH}_2)_2\text{NC}(\text{NC}_6\text{H}_3^1\text{Pr}_2\text{-}2,6)_2]_2\text{Y}_2(\mu_2\text{-Me})(\text{AlMe}_3)_2(\mu_4\text{-CH})$  (**1**) was obtained in 67% yield *via* a metal-assisted multiple C–H bond activation process when three equivalents of  $\text{AlMe}_3$  were added into a stirred toluene solution of the guanidinate yttrium bis(*o*-aminobenzyl) complex<sup>18</sup> at 60 °C for 18 h (Scheme 1). In order to get more insights into the formation process of the yttrium carbyne complex, the same reaction was carried out at room temperature for 6 h which gave a heterobimetallic Y/Al complex  $(\text{PhCH}_2)_2\text{NC}(\text{NC}_6\text{H}_3^1\text{Pr}_2\text{-}2,6)_2\text{Y}(\text{Me})(\text{AlMe}_4)$  (**2**) in 53% yield. It is interesting that complex **2** could turn into complex **1** in high yield in toluene at room temperature for 7 days with the release of  $\text{CH}_4$  (ESI Fig. S6<sup>†</sup>). This is sufficient to show that complex **2** is an intermediate in the formation of complex **1**.

The single crystal X-ray diffraction analysis of complex **1** shows that two distorted octahedral yttrium centers are linked by  $\mu_4\text{-CH}$  and  $\mu_2\text{-Me}$  units to form a distorted square while two  $\text{AlMe}_3$  groups work as bulky ligands to stabilize this binuclear carbyne complex (Fig. 1). The average Y–C1( $\mu_2\text{-Me}$ ) bond length (2.535(5) Å) is similar to that in  $[(\eta\text{-C}_5\text{H}_5)_2\text{YMe}]_2$  (2.537(9) Å).<sup>19a</sup>

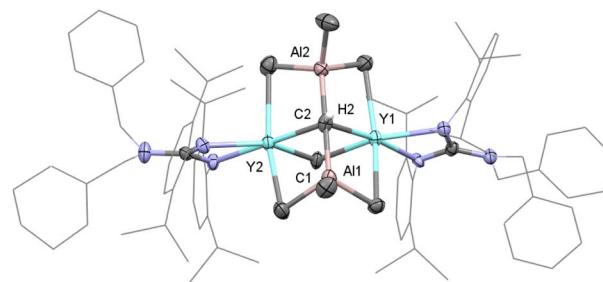
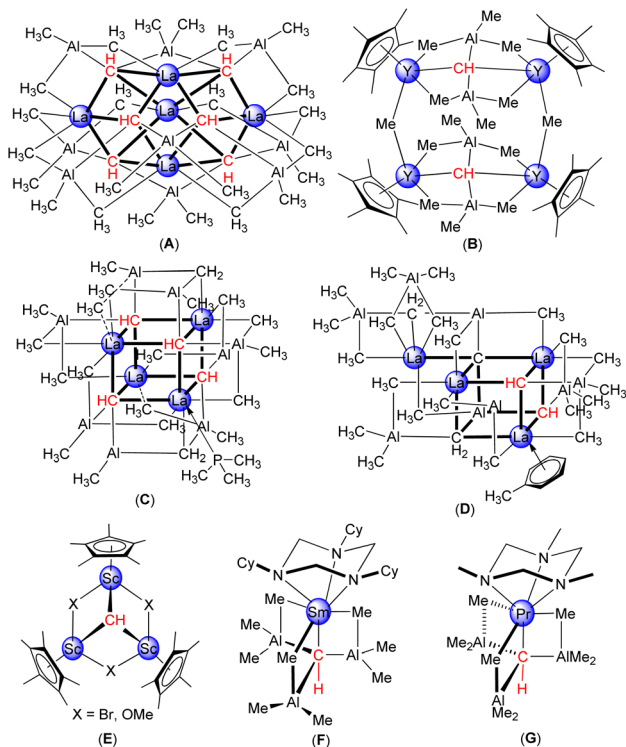


Fig. 1 Molecular structure of complex **1** with thermal ellipsoids at 30% probability except for the 2,6-( $^1\text{Pr}_2\text{C}_6\text{H}_3$  groups and benzyl groups in the guanidinate ligand. All of the hydrogen atoms (except for H2) are omitted for clarity. Selected bond distances (Å) and angles (°): Y(1)–C(1) 2.528(6), Y(1)–C(2) 2.418(5), Y(2)–C(1) 2.543(5), Y(2)–C(2) 2.398(5), C(2)–Al(1) 1.974(5), and C(2)–Al(2) 1.970(5); C(1)–Y(1)–C(2) 85.47(15), C(1)–Y(2)–C(2) 85.55(15), Y(1)–C(1)–Y(2) 91.29(17), and Y(1)–C(2)–Y(2) 97.65(16).

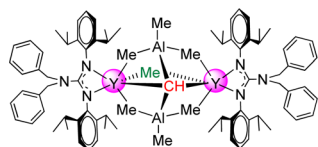
It is noticeable that the Y–C2( $\mu_4\text{-CH}$ ) bond lengths of 2.398(5) Å and 2.418(5) Å are shorter than those in  $[(\text{C}_5\text{Me}_5)\text{Y}(\mu_2\text{-Me})_2\text{-AlMe}_2]_2(\mu_2\text{-Me})(\mu_4\text{-CH})_2$  (2.444(3)–2.464(3) Å). A similar trend is observed for the Al–C2( $\mu_4\text{-CH}$ ) bond lengths (1.970(5) Å and 1.974(5) Å) *versus* 1.984(3)–1.993(3) Å for Al–C( $\mu_4\text{-CH}$ ),<sup>6a</sup> probably due to the steric hindrance. In the  $^1\text{H}$  NMR spectrum, the resonance of the  $[\text{CH}]^{3-}$  group is observed as a singlet at  $\delta = 2.36$  (benzene-*d*<sub>6</sub>) ppm, which is different to the proton signal at  $\delta = 12.16$  ppm in  $[(\text{C}_5\text{Me}_5)\text{Sc}(\mu_2\text{-Br})]_3(\mu_3\text{-CH})$ .<sup>8</sup> The metal-bonded  $\text{Y}_2\text{CHAl}_2$  methine carbon atom is shown at  $\delta = 90.2$  ppm based on a comprehensive analysis of the  $^1\text{H}$ ,  $^{13}\text{C}\{^1\text{H}\}$  and two-dimensional HMQC NMR spectra (Fig. S1–S3<sup>†</sup>). The bridged  $\mu_2\text{-Me}(\text{Y}–\text{Me}–\text{Y})$  and  $\text{AlMe}_3$  are shown as two singlets at  $\delta = -0.26$  and 0.34 ppm, respectively.

Complex **1** has good thermodynamic stability and multiple potential reactive sites (*e.g.*  $\mu_2\text{-methyl}$  and  $[\text{CH}]^{3-}$  groups) which makes this complex suitable for reactivity exploration. Complex **1** underwent a  $\sigma$ -bond metathesis reaction towards one equivalent of phenyl disulfide at room temperature, electron reduction of  $\text{PhSSPh}$  to form a  $(\text{SPh})^-$  anion moiety and release  $\text{PhSMe}$ , affording the yttrium thiolate-bridged carbyne complex  $[(\text{PhCH}_2)_2\text{NC}(\text{NC}_6\text{H}_3^1\text{Pr}_2\text{-}2,6)_2]_2\text{Y}_2(\mu_2\text{-SPh})(\text{AlMe}_3)_2(\mu_4\text{-CH})$  (**3**) in 86% isolated yield (Scheme 2). The molecular structure of **3** is

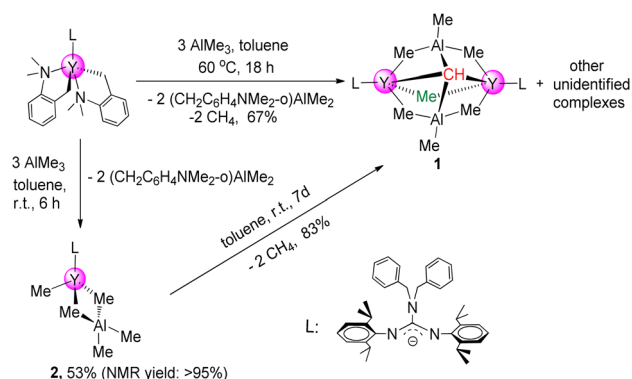
### Previous Works:



### This Work:



Scheme 1 Rare-earth-metal carbyne complexes.



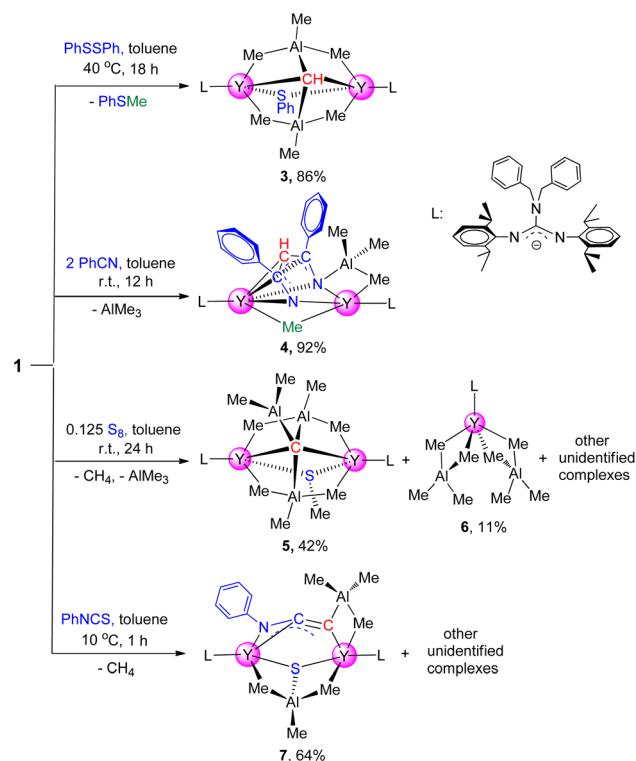
Scheme 2 Synthesis of binuclear yttrium carbyne complex **1**.



depicted in ESI Fig. S26†. Complex **3** is a dimer containing a  $\mu_2$ -SPh ligand, and the two Y–S bond lengths are 2.799(12) Å and 2.821(13) Å respectively, which are slightly shorter than those in  $[(C_5Me_5)_2Y(\mu-SPh)]_2$ ,<sup>20</sup> ranging from 2.893(6) to 2.903(6) Å, probably due to the steric hindrance. In the <sup>1</sup>H NMR spectrum, the distinct singlet at  $\delta = 2.00$  (benzene-*d*<sub>6</sub>) ppm is assigned to the  $[CH]^{3-}$  group, which is shifted to a high field compared to **1**. The methyl protons in the AlMe<sub>3</sub> unit split into two groups at  $\delta = 0.89$  and  $-0.50$  ppm at room temperature, while they become one broad peak at  $\delta = 0.51$  ppm at 60 °C (ESI Fig. S8†).<sup>19b</sup> Interestingly, the <sup>1</sup>H NMR monitoring of this reaction reveals that the chemoselectivity of the reaction of **1** with PhSSPh is independent of the amount of PhSSPh used, and no further reaction was observed even with an excess of PhSSPh.

To develop a synthetic methodology of metal *N*-heterocycle complexes from nitriles,<sup>21</sup> benzonitrile (2 equiv.) was added into the toluene solution of complex **1** at room temperature, obtaining a diinsertion product  $[(PhCH_2)_2NC(NC_6H_3^iPr_{2-2,6})_2Y_2(\mu_3-\eta^1:\eta^2:\eta^5-HC(CPhN)_2)(AlMe_3)(\mu_2-Me)]$  (**4**) in excellent yield as red blocks (Scheme 2). The X-ray single crystal diffraction study shows the structure of complex **4** in which the trianionic amino-alkenyl  $[CH(CPhN)_2]^{3-}$  unit acts as a pentadentate bridge ligand to connect two yttrium atoms in two bonding models ( $\eta^5$  and  $\eta^2$ ). In the NMR spectra, the  $[CH]^{3-}$  group appears as a singlet at  $\delta = 7.13$  ppm (<sup>13</sup>C: 96.5 ppm), which is shifted to a low field compared to **1** and **3**. The average C–N bond length of 1.319(5) Å is longer than the normal C=N double bond distance (1.26 Å),<sup>22</sup> while the C–C distance (av. 1.439(6) Å) is between the values observed for a C–C single bond and a C=C double bond, indicating that the three negative charges are delocalized partially in the  $[CH(CPhN)_2]^{3-}$  unit. It is interesting that the nucleophilic addition has only taken place on the single  $[CH]^{3-}$  group, and the bridged  $\mu_2$ -Me(Y–Me–Y) group is inert even if an excess amount of benzonitrile was used under the same conditions, or even heated up to 60 °C for 12 h. The results are clearly different from those of rare-earth-metal methylenide complexes, in which only monoinsertion products  $[PhC(NC_6H_3^iPr_{2-2,6})_2Ln_3(\mu_2-Me)_3(\mu_3-Me)[\mu-\eta^1:\eta^1:\eta^3-CH_2C(Ph)N]]$  (Ln = Y, Lu) were yielded.<sup>17c</sup> Additionally, the present reaction is also different from that of the scandium carbyne complex with PhCN, which afforded the monoaddition product  $[(C_5Me_5)Sc(\mu_2-OMe)]_3[\mu-\eta^2:\eta^2:\eta^3-CHC(Ph)N]^8$  possibly due to the steric hindrance and rigid structure.

Amazingly, the reaction of complex **1** with sulfur resulted in carbyne deprotonation to afford the rare carbide complex  $[(PhCH_2)_2NC(NC_6H_3^iPr_{2-2,6})_2Y_2(\mu_2-SMe)(AlMe_3)_2(\mu_5-C)(AlMe_2)]$  (**5**), along with the formation of the tetramethylaluminate complex  $[(PhCH_2)_2NC(NC_6H_3^iPr_{2-2,6})_2Y(AlMe_4)_2]$  (**6**) (Scheme 3). The single crystal structure of complex **5** reveals that the stabilization of the carbide unit (C<sup>4-</sup>) is achieved by the alkylaluminate ligands. The carbide carbon atom features a unique distorted trigonal bipyramidal geometry, in which three Al atoms lie in the equatorial plane and two Y atoms occupy the axial positions (ESI Fig. S28†). The bond length of Y–C7( $\mu_5$ -C) (av. 2.434(3) Å) is shorter than the Y–C( $\mu_6$ -C) in  $\{[(TMTAC)Y][Y_2(\mu_2-CH_3)]\}[(\mu_6-C)Al(\mu_2-CH_3)_2(CH_3)]_3\}(\mu_3-CH_2)(\mu_2-CH_3)Al(CH_3)_2\}_2$  (2.696(6) Å),<sup>23</sup> possibly due to higher coordination



Scheme 3 Reactions of complex **1** with benzonitrile, phenyl disulfide, sulfur and phenyl isothiocyanate.

numbers of the carbide atoms in latter. The results suggest that the elemental sulfur initiates a bimolecular reaction where the  $[CH]^{3-}$  group was deprotonated by the methyl in the AlMe<sub>3</sub> ligand to form a more stable carbide complex with the release of CH<sub>4</sub>.

Additionally, in order to expand the application of complex **1** as a nucleophile in the synthesis of rare-earth derivatives, the reaction of complex **1** with PhNCS was carried out. This reaction yields a yttrium sulfide complex  $[(PhCH_2)_2NC(NC_6H_3^iPr_{2-2,6})_2Y_2(\mu_3-\eta^1:\eta^2-CCNPh)(AlMe_3)_2(\mu_3-S)]$  (**7**) with a bridged ketenimine dianion unit (Scheme 3). The single crystal structure of complex **7** reveals that the N1–C1–C2 moiety displays a delocalized electronic framework, in which the C1–N1 (1.329(8) Å) bond length is intermediate between those of typical single and double bonds while the bond length of C1–C2 (1.221(8) Å) is slightly longer than the normal C≡C triple bond distance. And the average bond length of Y–S (2.660(17) Å) is longer than those in  $[(C_5Me_5)_2Y]_2(\mu-S)$  (2.54(5) Å)<sup>24</sup> probably due to the coordination of the AlMe<sub>3</sub> unit. The mechanism of this reaction is proposed to begin with PhNCS molecule insertion into the Y–C( $\mu_4$ -CH) bond, followed by isomerization to form a C=C double bond, and then C–S single bond cleavage takes place to give the final reductive coupling product **7** via C–H bond activation (ESI Fig. S33†). This result reveals the unique reactivity of the  $[CH]^{3-}$  group towards PhNCS, which is in sharp contrast with that of the cubane-type lutetium methylenide complex with PhNCS, which gave the corresponding ethylene amido thiolate/methylenide product through addition of a Lu–



methylidene bond with a less sterically demanding C=S bond followed by isomerization.<sup>11b</sup> The present reaction is also different from previous rare-earth-metal alkylidene complexes in cases where the fragments formed after the cleavage of the C=S double bond in PhNCS participate in the construction of the free coupled organic molecules.<sup>25</sup>

Carbon monoxide (CO), important C1 feedstock, insertion into metal-carbon bonds and its subsequent transformations were thought to play important roles in organometallic chemistry and industrial catalytic processes (Fischer-Tropsch synthesis).<sup>26</sup> However, the mechanistic details have not been fully understood at the molecular level; in consequence, the reaction of complex **1** with CO (1 atm) was examined at room temperature. Unfortunately, a complicated mixture is detected by using the <sup>1</sup>H NMR spectrum (ESI Fig. S22†). It is interesting that when the mixture was further heated to 50 °C for 18 h, an unexpected dioxo yttrium complex  $\{[(\text{PhCH}_2)_2\text{NC}(\text{NC}_6\text{H}_3^1\text{Pr}_2-2,6)_2]\text{Y}(\mu_3\text{-O})(\text{AlMe}_3)\}_2$  (**8**) was isolated in high yield as colorless crystals (Scheme 4). In the NMR spectra of **8**, only one singlet at  $\delta = -0.16$  ppm (<sup>13</sup>C = -2.6 ppm) was ascribed to AlMe<sub>3</sub> (ESI Fig. S18 and S19†). The X-ray single crystal diffraction study shows that two yttrium centers are linked by two oxygen atoms to form a distorted square in the dimeric system (ESI Fig. S31†), and the Y-O bond lengths (ranging from 2.122(3) to 2.207(2) Å) are comparable to those in (Tp<sup>Me2</sup>)<sub>3</sub>Y<sub>3</sub>(μ<sub>3</sub>-O)(μ<sub>2</sub>-O)(μ<sub>2</sub>-OCH<sub>2</sub>CH=CH<sub>2</sub>)(μ<sub>2</sub>-H) (from 2.127(2) to 2.268(19) Å).<sup>27</sup> To date, the reaction of CO with rare-earth-metal alkylidene complexes generated only rare-earth-metal ketene complexes through nucleophilic addition of an alkylidene group to CO.<sup>11b,13f</sup>

Although the CO deoxygenative coupling reaction induced by rare-earth-metal phosphinidene and polyhydrido complexes has been well documented,<sup>27,28</sup> the well-defined rare-earth-metal alkyl complex induced deoxygenative coupling reaction of CO was unprecedented. In order to offer more insight into the formation process of complex **8**, the same reaction was carried out in toluene at 10 °C for 6 h. To our delight, the yttrium mono-oxo complex  $[(\text{PhCH}_2)_2\text{NC}(\text{NC}_6\text{H}_3^1\text{Pr}_2-2,6)_2]\text{Y}_2(\mu_4\text{-O})(\text{AlMe}_3)_2(\mu_2\text{-Me})(\mu_2\text{-C}\equiv\text{CH})$  (**9**) was obtained in 84% isolated yield as colorless crystals (Scheme 4). According to single crystal

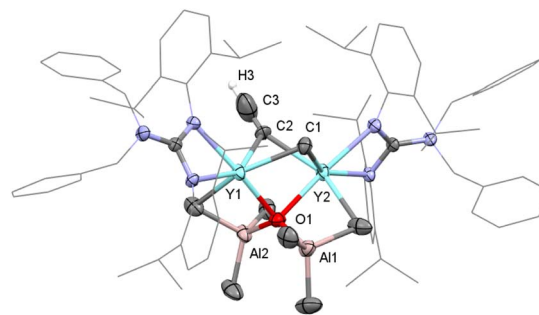


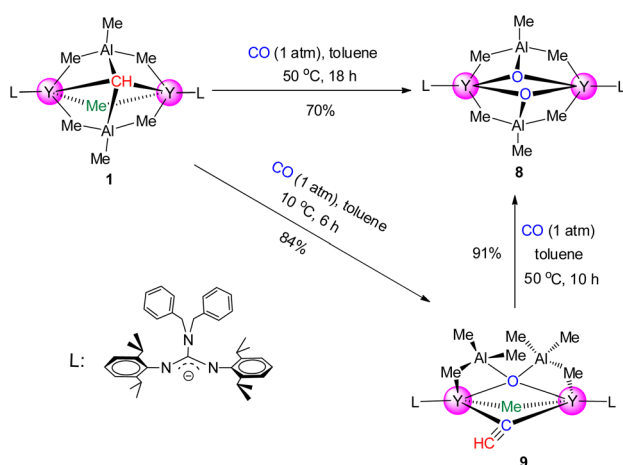
Fig. 2 Molecular structure of complex **9** with thermal ellipsoids at 30% probability except for the 2,6-(<sup>1</sup>Pr)<sub>2</sub>C<sub>6</sub>H<sub>3</sub> groups and benzyl groups in the guanidinate ligand. All of the hydrogen atoms (except for H3) are omitted for clarity. Selected bond distances (Å) and angles (°): Y(1)–C(1) 2.493(6), Y(1)–C(2) 2.537(6), Y(1)–O(1) 2.331(4), and C(2)–C(3) 1.065(12); Y(1)–C(1)–Y(2) 81.99(17), Y(1)–C(2)–Y(2) 84.13(18), Y(1)–O(1)–Y(2) 91.44(12), and Y(1)–C(2)–C(3) 118.1(7).

X-ray diffraction, the C2–C3 bond length (1.065(12) Å) reveals a substantial C≡C triple bond character (Fig. 2). And the NMR spectra of **9** show a singlet at  $\delta = 1.80$  ppm (<sup>13</sup>C{<sup>1</sup>H} = 112.4 ppm), which is regarded as bridged ethynyl (Fig. S17 and S18†). It's worth noting that complex **9** could turn into complex **8** almost quantitatively in toluene at 50 °C for 10 h, indicating that complex **9** is an intermediate in the formation of complex **8**. These reactions of CO may offer a convenient route to rare-earth-metal oxo complexes, a class of complexes that are of considerable current interest but still remain limited.<sup>27–29</sup>

### DFT calculations

The formation of complex **3** from complex **1** was investigated computationally at the DFT level (B3PW91 functional including dispersion). As can be seen from Fig. 3, the dispersion corrections play an important role to account for the reactivity due to the size of the substrate PhSSPh. Indeed, the coordination of the substrate is crucial in this case and implies the rearrangement of the μ<sub>2</sub>-Me(Y–Me–Y) to the terminal to allow the coordination of the substrate, which is only favored because of the dispersion forces (stabilization of 27.0 kcal mol<sup>−1</sup>). This is allowed to reach **TS5** where the methyl groups attack the sulfur inducing S–S bond breaking with an accessible barrier of 29.0 kcal mol<sup>−1</sup>. This barrier is in line with the experimental observation (18 h at 40 °C). Following the intrinsic reaction coordinate, it yields complex **3** whose formation is thermodynamically favorable (−59.4 kcal mol<sup>−1</sup>). The reaction cannot occur on the carbyne side as moving the carbyne to the top position is too unstable.

In addition, the formation of complex **9** from complex **1** was also investigated computationally. The computed enthalpy profile (Fig. 4) begins by the coordination of CO to one of the yttrium centers. This coordination is slightly exothermic by 17.2 kcal mol<sup>−1</sup>. From this adduct (**Int1**), the migratory insertion of CO onto the Y–CH bond is observed *via* **TS1**. The associated barrier is very low (6.4 kcal mol<sup>−1</sup>) in line with a facile insertion. Following the intrinsic reaction coordinate, it yields the insertion product (**Int2**) whose formation is exothermic by 10.0 kcal



Scheme 4 Reactions of complex **1** with CO.



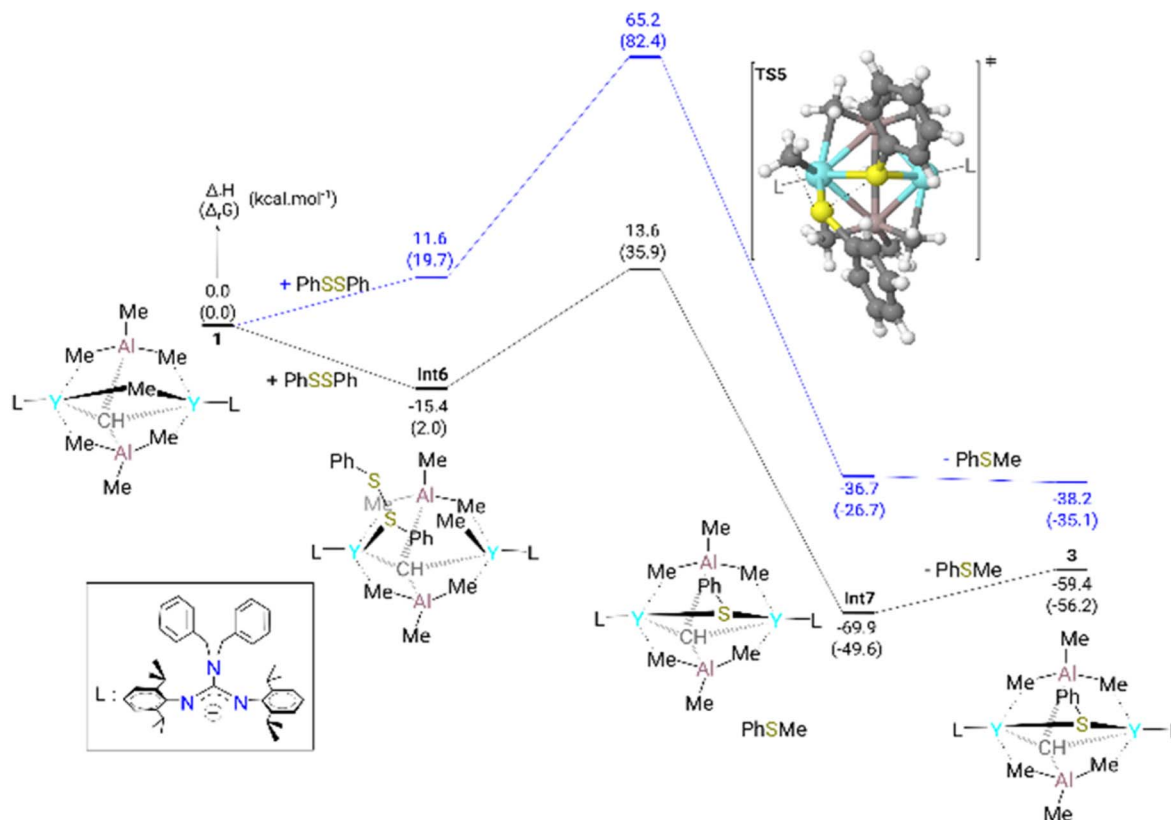


Fig. 3 Computed (DFT) enthalpy pathway of complex **3** at room temperature with (black) and without (blue) dispersion correction. The Gibbs free energies are given between brackets.

mol<sup>-1</sup> with respect to complex **1**. This intermediate will undergo an O–Al bond formation which is concomitant with C–Al bond breaking *via* **TS2**. The associated barrier is 6.5 kcal mol<sup>-1</sup> from **Int2** (13.7 kcal mol<sup>-1</sup> from complex **Int1**) and corresponds to the

rate-determining step of the entire transformation. This barrier height fits nicely the experimental conditions. **TS2** connects with **Int3**, whose formation is favorable (–29.9 kcal mol<sup>-1</sup>). **Int3** undergoes easy C–O bond breaking (**TS3**) with an enthalpy

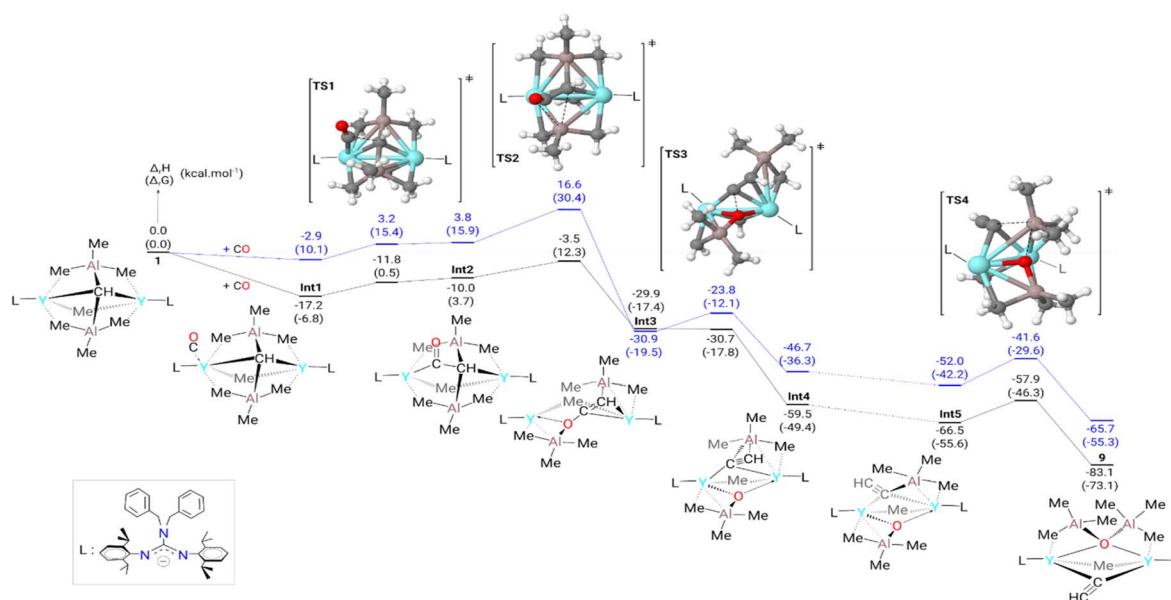


Fig. 4 Computed (DFT) enthalpy pathway of complex **9** at room temperature with (black) and without (blue) dispersion correction. The Gibbs free energies are given between brackets.



barrier of 0.2 kcal mol<sup>-1</sup>. This reaction yields a vinylidyne complex (**Int4**), with an extra stabilization of 29.6 kcal mol<sup>-1</sup> with respect to **Int3**. A rotamer of **Int4** (**Int5**) was located on the Potential Energy Surface (PES) with an enthalpy gain of 7.0 kcal mol<sup>-1</sup>. In the final step, the system undergoes C–Al bond formation with concomitant O–Al bond formation *via* **TS4**. The associated barrier is 8.6 kcal mol<sup>-1</sup> and allows the formation of complex **9**. The latter is found to be the most stable species of the whole reaction profile (–83.1 kcal mol<sup>-1</sup>). The addition of CO on the  $\mu_2$ -Me(Y–Me–Y) side was also computed and is higher in energy (ESI Fig. S34†).

## Conclusions

In summary, the first example of a well-defined binuclear carbyne complex **1** has been demonstrated. Complex **1** revealed diverse reactivity towards various substrates, such as nucleophilic addition with benzonitrile and phenyl isothiocyanate to form aza-allyl complex **4** and sulfide complex **7**,  $\sigma$ -bond metathesis towards phenyl disulfide to give thiolate complex **3**, and insertion of sulfide into the Y–C( $\mu_2$ -Me) bond along with carbyne deprotonation to afford carbide complex **5**. Unexpectedly, the rare-earth-metal carbyne complex induced deoxygenative coupling reaction of CO was also presented for the first time. The results have afforded some evidence to suggest that unsaturated substrates are attacked preferentially by the methine rather than the methyl. The observed rich reactivity of this binuclear carbyne complex could provide new insight into the nature of rare-earth-metal carbyne complexes. We are currently probing the reactivity of complex **1** with other molecules.

## Data availability

The data that support the findings of this study are available in the ESI† of this article.

## Author contributions

Li, Meng designed the carbyne complex. Jiang, Wen and Kong, Feng performed the synthetic experiment and X-ray diffraction measurements. Rosal, Iker del and Maron, Laurent performed the DFT calculations. Zhang, Lixin and Wang, Kai reviewed/revised the manuscript. All authors contributed to the analysis of the manuscript.

## Conflicts of interest

The authors declare no conflict of interest.

## Acknowledgements

This work was supported by the National Natural Science Foundation of China (grant no. 21871052 and 21672038). We thank Prof. Zhou Xigeng and Prof. Wang Huadong for their suggestions. The authors acknowledge the HPCs CALcul en Midi-Pyrénées (CALMIP-EOS grant 1415).

## Notes and references

- 1 E. O. Fischer, G. Kreis, C. G. Kreiter, J. Moller, G. Huttner and H. Lorenz, *Angew. Chem., Int. Ed. Engl.*, 1973, **12**, 564–565.
- 2 For examples of transition-metal alkylidyne complexes, see: (a) J. L. Polse, R. A. Andersen and R. G. Bergman, *J. Am. Chem. Soc.*, 1998, **120**, 13405–13414; (b) R. R. Schrock, *Chem. Rev.*, 2002, **102**, 145–179; (c) R. R. Schrock and A. H. Hoveyda, *Angew. Chem., Int. Ed.*, 2003, **42**, 4592–4633; (d) B. C. Bailey, A. R. Fout, H. Fan, J. Tomaszewski, J. C. Huffman and D. J. Mindiola, *Angew. Chem., Int. Ed.*, 2007, **46**, 8246–8249.
- 3 (a) M. Kamitani, B. Pinter, K. Searles, M. G. Crestani, A. Hickey, B. C. Manor, P. J. Carroll and D. J. Mindiola, *J. Am. Chem. Soc.*, 2015, **137**, 11872–11875; (b) J. Hillenbrand, M. Leutzsch and A. Fgrstner, *Angew. Chem., Int. Ed.*, 2019, **58**, 15690–15696; (c) A. Haack, J. Hillenbrand, M. Leutzsch, M. van Gastel, F. Neese and A. Fgrstner, *J. Am. Chem. Soc.*, 2021, **143**, 5643–5648; (d) S. Trzmiel, J. Langmann, D. Werner, C. Maichle-Mcßsmer, W. Scherer and R. Anwender, *Angew. Chem., Int. Ed.*, 2021, **60**, 20049–20054.
- 4 (a) P. F. Engel and M. Pfeffer, *Chem. Rev.*, 1995, **95**, 2281–2309; (b) M. J. Benedikter, F. Ziegler, J. Groos, P. M. Hauser, R. Schowner and M. R. Buchmeiser, *Coord. Chem. Rev.*, 2020, **415**, 213315; (c) M. Cui, H. H. Y. Sung, I. D. Williams and G. Jia, *J. Am. Chem. Soc.*, 2022, **144**, 6349–6360; (d) M. Cui and G. Jia, *J. Am. Chem. Soc.*, 2022, **144**, 12546–12566.
- 5 P. Zatsepin, E. Lee, J. Gu, M. R. Gau, P. J. Carroll, M. Baik and D. J. Mindiola, *J. Am. Chem. Soc.*, 2020, **142**, 10143–10152.
- 6 (a) H. M. Dietrich, H. Grove, K. W. Törnroos and R. Anwender, *J. Am. Chem. Soc.*, 2006, **128**, 1458–1459; (b) L. C. H. Gerber, E. Le Roux, K. W. Törnroos and R. Anwender, *Chem.–Eur. J.*, 2008, **14**, 9555–9564.
- 7 (a) D. Bojer, A. Venugopal, B. Neumann, H.-G. Stammler and N. W. Mitzel, *Angew. Chem., Int. Ed.*, 2010, **49**, 2611–2614; (b) D. Bojer, B. Neumann, H.-G. Stammler and N. W. Mitzel, *Chem.–Eur. J.*, 2011, **17**, 6239–6247; (c) D. Bojer, B. Neumann, H.-G. Stammler and N. W. Mitzel, *Eur. J. Inorg. Chem.*, 2011, 3791–3796.
- 8 P. Deng, X. Shi, X. Gong and J. Cheng, *Chem. Commun.*, 2021, 57, 6436–6439.
- 9 (a) K. Aparna, M. Ferguson and R. G. Cavell, *J. Am. Chem. Soc.*, 2000, **122**, 726–727; (b) D. P. Mills, L. Soutar, W. Lewis, A. J. Blake and S. T. Liddle, *J. Am. Chem. Soc.*, 2010, **132**, 14379–14381; (c) M. Fustier, X. F. Le Goff, P. Le Floch and N. Mézailles, *J. Am. Chem. Soc.*, 2010, **132**, 13108–13110; (d) S. T. Liddle, D. P. Mills and A. J. Wooles, *Chem. Soc. Rev.*, 2011, **40**, 2164–2176; (e) M. Fustier, X. F. Le Goff, M. Lutz, J. C. Slootweg and N. Mézailles, *Organometallics*, 2015, **34**, 63–72.
- 10 (a) H. M. Dietrich, K. W. Törnroos and R. Anwender, *J. Am. Chem. Soc.*, 2006, **128**, 9298–9299; (b) M. Zimmermann, J. Takats, G. Kiel, K. W. Törnroos and R. Anwender, *Chem. Commun.*, 2008, 612–614; (c) M. Zimmermann, D. Rauschmaier, K. Eichele, K. W. Törnroos and



- R. Anwander, *Chem. Commun.*, 2010, **46**, 5346–5348; (d) C. O. Hollfelder, L. N. Jende, H. M. Dietrich, K. Eichele, C. Maichle-Mössmer and R. Anwander, *Chem.–Eur. J.*, 2019, **25**, 7298–7302; (e) D. Barisic, D. Diether, C. Maichle-Mössmer and R. Anwander, *J. Am. Chem. Soc.*, 2019, **141**, 13931–13940; (f) C. O. Hollfelder, M. Zimmermann, C. Spiridopoulos, D. Werner, K. W. Törnroos, C. Maichle-Mössmer and R. Anwander, *Molecules*, 2019, **24**, 3703–3730; (g) D. A. Buschmann, L. Schumacher and R. Anwander, *Chem. Commun.*, 2022, **58**, 9132–9135.
- 11 (a) W. Zhang, Z. Wang, M. Nishiura, Z. Xi and Z. Hou, *J. Am. Chem. Soc.*, 2011, **133**, 5712–5715; (b) T. Li, M. Nishiura, J. Cheng, Y. Li and Z. Hou, *Chem.–Eur. J.*, 2012, **18**, 15079–15085.
- 12 (a) J. Scott, H. J. Fan, B. F. Wicker, A. R. Fout, M. H. Baik and D. J. Mindiola, *J. Am. Chem. Soc.*, 2008, **130**, 14438–14439; (b) R. Litlabø, M. Zimmermann, K. Saliu, J. Takats, K. W. Törnroos and R. Anwander, *Angew. Chem., Int. Ed.*, 2008, **47**, 9560–9564; (c) P. Zatsepin, E. Lee, J. Gu, M. R. Gau, P. J. Carroll, M. Baik and D. J. Mindiola, *J. Am. Chem. Soc.*, 2020, **142**, 10143–10152.
- 13 (a) S. Li, M. Wang, B. Liu, L. Li, J. Cheng, C. Wu, D. Liu, J. Liu and D. Cui, *Chem.–Eur. J.*, 2014, **20**, 15493–15498; (b) T. Li, G. Zhang, J. Guo, S. Wang, X. Leng and Y. Chen, *Organometallics*, 2016, **35**, 1565–1572; (c) F. Yan, S. Li, L. Li, W. Zhang, D. Cui, M. Wang and Y. Dou, *Eur. J. Inorg. Chem.*, 2019, 2277–2283.
- 14 (a) W. Ma, C. Yu, Y. Chi, T. Chen, L. Wang, J. Yin, B. Wei, L. Xu, W. Zhang and Z. Xi, *Chem. Sci.*, 2017, **8**, 6852–6856; (b) Y. Zheng, C. Cao, W. Ma, T. Chen, B. Wu, C. Yu, Z. Huang, J. Yin, H. Hu, J. Li, W. Zhang and Z. Xi, *J. Am. Chem. Soc.*, 2020, **142**, 10705–10714; (c) Z. Lv, Z. Chai, M. Zhu, J. Wei and W. Zhang, *J. Am. Chem. Soc.*, 2021, **143**, 9151–9161; (d) Z. Lv, W. Liu, M. Zhu, Z. Chai, J. Wei and W. Zhang, *Chem.–Eur. J.*, 2021, **27**, 16498–16504.
- 15 (a) D. J. Mindiola and J. Scott, *Nat. Chem.*, 2011, **3**, 15–17; (b) W. Mao, L. Xiang, C. A. Lamsfus, L. Maron, X. Leng and Y. Chen, *J. Am. Chem. Soc.*, 2017, **139**, 1081–1084; (c) W. Mao, L. Xiang, L. Maron, X. Leng and Y. Chen, *J. Am. Chem. Soc.*, 2017, **139**, 17759–17762; (d) C. Wang, W. Mao, L. Xiang, Y. Yang, J. Fang, L. Maron, X. Leng and Y. Chen, *Chem.–Eur. J.*, 2018, **24**, 13903–13917; (e) W. Q. Mao, L. Xiang, C. A. Lamsfus, L. Maron, X. Leng and Y. Chen, *Chin. J. Chem.*, 2018, **36**, 904–908; (f) W. Mao, Y. Wang, L. Xiang, Q. Peng, X. Leng and Y. Chen, *Chem.–Eur. J.*, 2019, **25**, 10304–10308.
- 16 J. Hong, L. Zhang, X. Yu, M. Li, Z. Zhang, P. Zheng, M. Nishiura, Z. Hou and X. Zhou, *Chem.–Eur. J.*, 2011, **17**, 2130–2137.
- 17 (a) J. Hong, L. Zhang, K. Wang, Y. Zhang, L. Weng and X. Zhou, *Chem.–Eur. J.*, 2013, **19**, 7865–7873; (b) K. Wang, G. Luo, J. Hong, X. Zhou, H. Weng, Y. Luo and L. Zhang, *Angew. Chem., Int. Ed.*, 2014, **53**, 1053–1056; (c) J. Hong, Z. Li, Z. Chen, L. Weng, X. Zhou and L. Zhang, *Dalton Trans.*, 2016, **45**, 6641–6649; (d) J. Hong, H. Tian, L. Zhang, X. Zhou, I. del Rosal, L. Weng and L. Maron, *Angew. Chem., Int. Ed.*, 2018, **57**, 1062–1067; (e) H. Tian, J. Hong, K. Wang, I. Rosal, L. Maron, X. Zhou and L. Zhang, *J. Am. Chem. Soc.*, 2018, **140**, 102–105.
- 18 F. Kong, M. Li, X. Zhou and L. Zhang, *RSC Adv.*, 2017, **7**, 29752–29761.
- 19 (a) J. Holton, M. F. Lappert, D. G. H. Ballard, R. Pearce, J. L. Atwood and W. E. Hunter, *J. Chem. Soc., Dalton Trans.*, 1979, 54–61; (b) R. Litlabø, M. Zimmermann, K. Saliu, J. Takats, K. W. Törnroos and R. Anwander, *Angew. Chem., Int. Ed.*, 2008, **47**, 9560–9564.
- 20 W. J. Evans, B. M. Schmiede, S. E. Lorenz, K. A. Miller, T. M. Champagne, J. W. Ziller, A. G. DiPasquale and A. L. Rheingold, *J. Am. Chem. Soc.*, 2008, **130**, 8555–8563.
- 21 (a) R. A. Michelin, M. Mozzon and R. Bertani, *Coord. Chem. Rev.*, 1996, **147**, 299–338; (b) V. Y. Kukushkin and A. J. L. Pombeiro, *Chem. Rev.*, 2002, **102**, 1771–1802; (c) H. Wu and N. K. Devaraj, *Acc. Chem. Res.*, 2018, **51**, 1249–1259.
- 22 G. Häfelinger, MO- $\pi$ -Bindungsordnung-Bindungslängen-Beziehungen-für Hetero- $\pi$ -Systeme, I.  $\pi$ -Systememit CN-Bindungen, *Chem. Ber.*, 1970, **103**, 2902–2921.
- 23 A. Venugopal, I. Kamps, D. Bojer, R. J. F. Berger, A. Mix, A. Willner, B. Neumann, H.-G. Stammer and N. W. Mitzel, *Dalton Trans.*, 2009, 5755–5765.
- 24 M. E. Fieser, C. W. Johnson, J. E. Bates, J. W. Ziller, F. Furche and W. J. Evans, *Organometallics*, 2015, **34**, 4387–4393.
- 25 (a) D. P. Mills, L. Soutar, O. J. Cooper, W. Lewis, A. J. Blake and S. T. Liddle, *Organometallics*, 2013, **32**, 1251–1264; (b) D. P. Mills, W. Lewis, A. J. Blake and S. T. Liddle, *Organometallics*, 2013, **32**, 1239–1250.
- 26 (a) C. K. Rofer-Depoorter, *Chem. Rev.*, 1981, **81**, 447–474; (b) J. P. Collmann, L. S. Hege, J. R. Norton and R. G. Finke, *Principles and Applications of Organotransition Metal Chemistry*, University Science Book, Mill Valley, CA, 1987; (c) P. L. Arnold and Z. R. Turner, *Nat. Rev. Chem.*, 2017, **1**, 0002.
- 27 J. Cheng, M. J. Ferguson and J. Takats, *J. Am. Chem. Soc.*, 2010, **132**, 2–3.
- 28 (a) T. Shima and Z. Hou, *J. Am. Chem. Soc.*, 2006, **128**, 8124–8125; (b) Y. Takenaka, T. Shima, J. Baldamus and Z. Hou, *Angew. Chem., Int. Ed.*, 2009, **48**, 7888–7891; (c) Y. Lv, C. E. Kefalidis, J. Zhou, L. Maron, X. Leng and Y. Chen, *J. Am. Chem. Soc.*, 2013, **135**, 14784–14796.
- 29 (a) W. J. Evans, J. W. Grate, I. Bloom, W. E. Hunter and J. L. Atwood, *J. Am. Chem. Soc.*, 1985, **107**, 405–409; (b) O. Tardif, D. Hashizume and Z. Hou, *J. Am. Chem. Soc.*, 2004, **126**, 8080–8081; (c) J. Scott, H. Fan, B. F. Wicker, A. R. Fout, M. H. Baik and D. J. Mindiola, *J. Am. Chem. Soc.*, 2008, **130**, 14438–14439; (d) M. Fustier, X. F. Le Goff, P. Le Floch and N. Mézailles, *J. Am. Chem. Soc.*, 2010, **132**, 13108–13110; (e) P. L. Arnold, E. Hollis, F. J. White, N. Magnani, R. Caciuffo and J. B. Love, *Angew. Chem., Int. Ed.*, 2011, **50**, 887–890; (f) W. Zhang, Z. Wang, M. Nishiura, Z. Xi and Z. Hou, *J. Am. Chem. Soc.*, 2011, **133**, 5712–5715; (g) P. L. Damon, G. Wu, N. Kaltsoyannis and T. W. Hayton, *J. Am. Chem. Soc.*, 2016, **138**, 12743–12746.

